Vol. 4 No. 3 JOURNAL OF COMPUTATIONAL MATHEMATICS July 1986

VARIABLE-ELLIPTIC-VORTEX METHOD FOR INCOMPRESSIBLE FLOW SIMULATION*[1]

TENG ZHEN-HUAN (滕振寰)

(Peking University, Beijing, China)

Abstract

A variable-elliptic-vortex method, which is a generalization of the elliptic-vortex method proposed by the author in [1], is presented for the numerical simulation of incompressible flows. The most attractive feature of the new method is that the numerical vortex blobs used in this model like actual vortex blobs can be translated, rotated and deformed in elliptic shape. The new method provides a more reasonable and more accurate approach for flow simulation than the fixed-vortex methods. Numerical examples are presented to demonstrate the performance of the new method.

§1. Introduction

Vortex methods have provided an attractive and successful approach for the numerical simulation of incompressible fluid flows at high Reynolds number. The features of these methods are as follows: (1) the interactions of the numerical vortices mimic the physical mechanisms in actual fluid flow; (2) vortex methods are automatically adaptive, since the vortex "blobs" concentrate in the regions of physical interest; and (3) there are no inherent errors with behavior like the numerical viscosity of Eulerian difference methods. Such numerical viscosity often obscures the effects of physical viscosity in high Reynolds number flow simulation.

The first attempts by Rosenhead [2] to simulate flows by a vortex method used point vortices. But the point vortex method introduces a singularity of the velocity field in its centre. Chorin [3] and Kuwahara and Takami [4] introduced a vortex method with finite cores or vortex blobs, to smooth out the singularity and to stabilize the method. There have been a large number of successful flow simulations by vortex blob methods (see Leonard [5]).

It is however noticed that up to now all of the numerical vortex blobs in use are assumed to retain fixed shape for all time while the actual flow can undergo substantial distortion. The "unphysical behavior" of vortex blobs reduces the accuracy of the vortex methods, even though it does not interfere with the convergence of vortex methods ([6], [7], [13]). Thus there is considerable interest in finding an appropriate approach to form a method with variable vortex blobs, which can follow the distortion of actual vortex blobs.

In this paper a variable-elliptic-vortex method is presented to meet this need, which is a generalization of the elliptic-vortex method proposed by the author in [1]. The most attractive feature of the new model is that the variable vortex blobs

* Received July 18, 1985.

1) This work was supported by the Science Fund of the Chinese Education Ministry.

can be translated, rotated and deformed in the shape of elliptic type according to the decomposition theorem of velocity in a small neighborhood. The main merits of the new model are as follows: (1) it provides a more flexible and more reasonable approach to mimic physical flows; (2) it has higher order accuracy in space than the fixed shape vortex method.

§ 2. Approximate Motion of a Small Elliptic Blob

In this paper we are mainly concerned with incompressible inviscid flows in two dimensions satisfying the Euler equations in the vortex form

$$\begin{cases} \dfrac{\partial \xi}{\partial t}+u\dfrac{\partial \xi}{\partial x}+v\dfrac{\partial \xi}{\partial y}=0, \\ \Delta\psi=-\xi, \\ u=\dfrac{\partial \psi}{\partial y},\ v=-\dfrac{\partial \psi}{\partial x}, \end{cases} \tag{1}$$

where $\boldsymbol{u}=(u, v)$ is the velocity vector, $\boldsymbol{r}=(x, y)$ is the position, t is the time, ψ is the stream function, $\xi=\dfrac{\partial v}{\partial x}-\dfrac{\partial u}{\partial y}$ is the vorticity, $\Delta\equiv\nabla^2$ is the Laplace operator.

In the following we consider an approximate motion of a small blob Ω_0 in fluid. Let Ω_0 be an elliptic blob at $t=0$ centred at $\boldsymbol{a}_0=(\alpha_{10}, \alpha_{20})$ defined by

$$\Omega_0=\{\boldsymbol{\alpha}\,|\,(\boldsymbol{\alpha}-\boldsymbol{a}_0)A(\boldsymbol{\alpha}-\boldsymbol{a}_0)^T\leqslant 1,\ \boldsymbol{\alpha}\in\mathbb{R}^2\},$$

where $A=(a_{ij})$ is a 2×2 positive definite matrix. A small elliptic blob Ω_0 means that its major axis is small.

We will use $\boldsymbol{\alpha}=(\alpha_1, \alpha_2)$ for the Lagrangian coordinates of a fluid particle. Thus a particle starting at the position $\boldsymbol{\alpha}\in\Omega_0$ at $t=0$ follows a trajectory $\boldsymbol{r}(t;\ \boldsymbol{\alpha})$ determined by the equation

$$\begin{cases} \dfrac{d\boldsymbol{r}}{dt}=\boldsymbol{u}(\boldsymbol{r}, t), \\ \boldsymbol{r}(0;\ \boldsymbol{\alpha})=\boldsymbol{\alpha}. \end{cases} \tag{2}$$

In writing equations to approximate (2), we expand $\boldsymbol{u}(\boldsymbol{r}, t)$ at $\boldsymbol{r}_0(t)=\boldsymbol{r}(t;\ \boldsymbol{a}_0)$, the trajectory of the center $\boldsymbol{a}_0$ of Ω_0, by Taylor's theorem

$$\boldsymbol{u}(\boldsymbol{r}, t)=\boldsymbol{u}(\boldsymbol{r}_0, t)+(\boldsymbol{r}-\boldsymbol{r}_0)\cdot\nabla\boldsymbol{u}(\boldsymbol{r}_0, t)^T+O(|\boldsymbol{r}-\boldsymbol{r}_0|^2),$$

where $\nabla\boldsymbol{u}=\begin{pmatrix} \partial_x u & \partial_y u \\ \partial_x v & \partial_y v \end{pmatrix}$ denotes the Jacobian matrix of $\boldsymbol{u}$ and $(\boldsymbol{r}-\boldsymbol{r}_0)\cdot\nabla\boldsymbol{u}(\boldsymbol{r}_0, t)^T$ is a matrix multiplication. Substituting the expression into (2) and neglecting the term of $O(|\boldsymbol{r}-\boldsymbol{r}_0|^2)$, we get an approximate system

$$\frac{d\boldsymbol{r}}{dt}=\boldsymbol{u}(\boldsymbol{r}_0, t)+(\boldsymbol{r}-\boldsymbol{r}_0)\cdot\nabla\boldsymbol{u}(\boldsymbol{r}_0, t)^T \tag{3}$$

which is a linear ordinary differential system if $\boldsymbol{r}_0(t)$ is assumed to be a known trajectory. From above we know that (3) approximates (2) with second order accuracy in space. In using notations of $\boldsymbol{z}=\boldsymbol{r}-\boldsymbol{r}_0$ and $\boldsymbol{\beta}=\boldsymbol{\alpha}-\boldsymbol{a}_0$, (3) becomes

$$\begin{cases} \dfrac{dz}{dt} = z \cdot \nabla u(r_0, t)^T, \\ z(0; \beta) = \beta, \end{cases} \tag{4}$$

where $\beta \in \Omega_0 = \{\beta \mid \beta A \beta^T \leqslant 1,\ \beta \in \mathbb{R}^2\}$. We denote the solution of the ordinary differential system by $z(t; \beta) = \phi^t(\beta)$; thus the approximate motion of Ω_0 can be expressed by $\Omega(t) = \phi^t(\Omega_0)$.

From the linear system theory[8], we know that the solution of (4) can be written in

$$z(t; \beta) = \beta Z(t), \tag{5}$$

where $Z(t)$ is a 2×2 fundamental matrix of (4) with

$$Z(0) = E,$$

E being a unitary matrix. According to the Liouville theorem[8], we have

$$\det Z(t) = \det Z(0) \exp \int_0^t \operatorname{tr} \nabla u(r_0, t)^T dt = \det Z(0) \exp \int_0^t \operatorname{div} u(r_0, t) dt.$$

In view of $Z(0) = E$ and incompressibility $\operatorname{div} u = 0$, we get

$$\det Z(t) = 1.$$

Substituting (5) into Ω_0, one gets the expression of the approximate motion of Ω_0

$$\Omega(t) = \{z \mid z Z^{-1}(t) A (Z^{-1}(t))^T z^T \leqslant 1,\ z \in \mathbb{R}^2\}. \tag{6}$$

A simple calculation shows that $A(t) \equiv Z^{-1}(t) A (Z^{-1}(t))^T$ is a positive definite matrix and its determinant is constant, i.e. $\det A(t) = \det A$. This implies that $\Omega(t)$ is deformed in the elliptic shape and its area is invariant in time. So we arrive at the following conclusion:

Proposition. If the motion of a small elliptic blob Ω_0 is approximated by the second order accuracy system (3), then the approximate motion of Ω_0 is the sum of a (rigid) translation following its center trajectory $r_0(t)$ and a distortion in the elliptic shape (6) with conserved area.

§ 3. Variable Elliptic Vortex Model

To solve Euler equations (1), suppose the vorticity field is now represented by the sum of elliptic vortex blobs ξ_j

$$\xi(x, y, t) = \sum_{j=1}^{N} \xi_j(x, y, t). \tag{7}$$

The elliptic vortices ξ_j are defined by

$$\xi_j(x, y, t) = \Gamma_j \gamma(x, y; \Omega_j(t)), \tag{8}$$

where Γ_j are their respective circulation, γ is a uniform vorticity distribution over an ellipse $\Omega_j(t)$, which is given by

$$\gamma(x, y; \Omega_j(t)) = \begin{cases} \dfrac{1}{\sigma_j}, & (x, y) \in \Omega_j(t), \\ 0, & (x, y) \notin \Omega_j(t). \end{cases}$$

Here σ_j is the area of $\Omega_j(t)$ and the ellipse $\Omega_j(t)$ is defined by

$$\Omega_j(t) = \{r \mid (r - r_j(t)) A_j(t) (r - r_j(t))^T \leqslant 1,\ r \in \mathbb{R}^2\},$$

where $A_j(t)$ is a 2×2 positive definite matrix and $\boldsymbol{r}_j(t)=(x_j(t), y_j(t))$ is the center of $\Omega_j(t)$.

It follows from the results of [1] that the induced velocity field by the vorticity field (7) can be explicitly expressed as

$$\boldsymbol{u}(\boldsymbol{r}, t)=\sum_{j=1}^{N} \Gamma_j\left(\frac{\partial}{\partial y}, -\frac{\partial}{\partial y}\right)\phi(x, y; \Omega_j(t)), \tag{9}$$

where

$$\frac{\partial}{\partial x}\phi=\begin{cases}\dfrac{1}{\pi(a_j+b_j)}\left(\dfrac{X_j\cos\theta_j}{a_j}+\dfrac{-Y_j\sin\theta_j}{b_j}\right), & (x, y)\in\Omega_j(t),\\ \dfrac{1}{\pi(\alpha_j+\beta_j)}\left(\dfrac{X_j\cos\theta_j}{\alpha_j}+\dfrac{-Y_j\sin\theta_j}{\beta_j}\right), & (x, y)\overline{\in}\Omega_j(t),\end{cases} \tag{10a}$$

$$\frac{\partial}{\partial y}\phi=\begin{cases}\dfrac{1}{\pi(a_j+b_j)}\left(\dfrac{X_j\sin\theta_j}{a_j}+\dfrac{Y_j\cos\theta_j}{b_j}\right), & (x, y)\in\Omega_j(t),\\ \dfrac{1}{\pi(\alpha_j+\beta_j)}\left(\dfrac{X_j\sin\theta_j}{\alpha_j}+\dfrac{Y_j\cos\theta_j}{\beta_j}\right), & (x, y)\overline{\in}\Omega_j(t),\end{cases} \tag{10b}$$

$$X_j=(x-x_j)\cos\theta_j+(y-y_j)\sin\theta_j, \tag{10c}$$

$$Y_j=-(x-x_j)\sin\theta_j+(y-y_j)\cos\theta_j,$$

$$\alpha_j=\sqrt{a_j^2+\lambda_j}, \quad \beta_j=\sqrt{b_j^2+\lambda_j}, \tag{10d}$$

and $\lambda_j(>0)$ satisfies

$$\frac{X_j^2}{(a_j^2+\lambda_j)}+\frac{Y_j^2}{(b_j^2+\lambda_j)}=1. \tag{10e}$$

In the above expressions, a_j, b_j are the major and minor axis of $\Omega_j(t)$ respectively, and θ_j is the included angle of the major axis a_i with x-axis. Recalling analytical geometry we know that these parameters can be determined by the components of $A_j(t)=\begin{pmatrix} a_{11}^{(j)}, & a_{12}^{(j)} \\ a_{21}^{(j)}, & a_{22}^{(j)}\end{pmatrix}$ in the following way

$$\begin{aligned}&\operatorname{tg}\theta_j=-\left(\frac{a_{11}^{(j)}-a_{22}^{(j)}}{2a_{12}^{(j)}}+\sqrt{\frac{(a_{11}^{(j)}-a_{22}^{(j)})^2}{2a_{12}^{(j)}}+1}\right),\\ &\gamma_j=\sqrt{\frac{a_{11}^{(j)}+2a_{12}^{(j)}\operatorname{tg}\theta_j+a_{22}^{(j)}\operatorname{tg}^2\theta_j}{a_{11}^{(j)}\operatorname{tg}^2\theta_j-2a_{12}^{(j)}\operatorname{tg}\theta_j+a_{22}^{(j)}}},\\ &a_j=\sqrt{\frac{\sigma_j}{\pi\gamma_j}}, \quad b_j=\sqrt{\frac{\sigma_j\gamma_j}{\pi}},\end{aligned} \tag{10f}$$

where $\sigma_j=\det A_j$.

The formulas given above show that once the motions of the elliptic blobs $\Omega_j(t)$ $\{j=1, \cdots, N\}$ are known the velocity field can be explicitly solved by (9). Based on the results in the previous section we will use system (3) to approximate $\Omega_j(t)$. To this end replacing $\boldsymbol{r}_0(t)$ in (3) and (4) with $\boldsymbol{r}_j(t)$, one gets the equations of the fundamental matrix Z_j

$$\begin{cases}\dfrac{dZ_j}{dt}=Z_j\cdot\nabla\boldsymbol{u}(\boldsymbol{r}_j(t), t)^T,\\ Z_j|_{t=0}=E, \quad j=1, 2, \cdots, N,\end{cases} \tag{11}$$

where the center trajectories $\boldsymbol{r}_j(t)$ of $\Omega_j(t)$ are described by

$$\begin{cases} \dfrac{d\boldsymbol{r}_j}{dt}=\boldsymbol{u}(\boldsymbol{r}_j(t),\,t), \\ \boldsymbol{r}_j|_{t=0}=\boldsymbol{r}_j(0), \quad j=1,\,2,\,\cdots,\,N, \end{cases} \tag{12}$$

$\boldsymbol{r}_j(0)$ being the initial center of $\Omega_j(t)$. In the above $\boldsymbol{u}(\boldsymbol{r}_j(t),\,t)$ is given by (9) and $\nabla\boldsymbol{u}(\boldsymbol{r}_j(t),t)$ is also derived from (9) as follows:

$$\begin{aligned} &\frac{\partial}{\partial x}u(\boldsymbol{r},\,t)=-\sum_{j=1}^{N}\Gamma_j\frac{\partial^2}{\partial x\,\partial y}\phi(x,\,y;\,\Omega_j(t)), \\ &\frac{\partial}{\partial y}u(\boldsymbol{r},\,t)=-\sum_{j=1}^{N}\Gamma_j\frac{\partial^2}{\partial y^2}\phi(x,\,y;\,\Omega_j(t)), \\ &\frac{\partial}{\partial x}v(\boldsymbol{r},\,t)=-\xi(\boldsymbol{r},\,t)+\frac{\partial}{\partial y}u(\boldsymbol{r},\,t)=-\sum_{j=1}^{N}\Gamma_j\gamma(x,\,y;\,\Omega_j(t))+\frac{\partial}{\partial y}u(\boldsymbol{r},\,t), \\ &\frac{\partial}{\partial y}v(\boldsymbol{r},\,t)=-\frac{\partial}{\partial x}u(\boldsymbol{r},\,t), \end{aligned} \tag{13}$$

where

$$\frac{\partial^2}{\partial x\,\partial y}\phi=\begin{cases} \dfrac{1}{\pi(a_j+b_j)}\left(\dfrac{1}{a_j}-\dfrac{1}{b_j}\right)\sin\theta_j\cos\theta_j, & (x,\,y)\in\Omega_j, \\ \dfrac{1}{\pi(\alpha_j+\beta_j)}\left(\dfrac{1}{\alpha_j}-\dfrac{1}{\beta_j}\right)\sin\theta_j\cos\theta_j-\dfrac{1}{\pi\alpha_j\beta_j} \\ \quad\times\dfrac{\left(\dfrac{X_j\cos\theta_j}{\alpha_j^2}-\dfrac{Y_j\sin\theta_j}{\beta_j^2}\right)\left(\dfrac{X_j\sin\theta_j}{\alpha_j^2}+\dfrac{Y_j\cos\theta_j}{\beta_j^2}\right)}{\dfrac{X_j^2}{\alpha_j^4}+\dfrac{Y_j^2}{\beta_j^4}}, & (x,\,y)\overline{\in}\Omega_j, \end{cases} \tag{14a}$$

$$\frac{\partial^2}{\partial y^2}\phi=\begin{cases} \dfrac{1}{\pi(a_j+b_j)}\left(\dfrac{\sin^2\theta_j}{a_j}+\dfrac{\cos^2\theta_j}{b_j}\right), & (x,\,y)\in\Omega_j, \\ \dfrac{1}{\pi(\alpha_j+\beta_j)}\left(\dfrac{\sin^2\theta_j}{\alpha_j}+\dfrac{\cos^2\theta_j}{\beta_j}\right)-\dfrac{1}{\pi\alpha_j\beta_j}\dfrac{\left(\dfrac{X_j\sin\theta_j}{\alpha_j^2}+\dfrac{Y_j\cos\theta_j}{\beta_j^2}\right)^2}{\dfrac{X_j^2}{\alpha_j^4}+\dfrac{Y_j^2}{\beta_j^4}}, & (x,\,y)\overline{\in}\Omega_j \end{cases} \tag{14b}$$

and the parameters a_j, b_j, $\cdots$ are given in (10c)—(10f). As showed in Section 1 the approximate motion of $\Omega_j(t)$ can be expressed as

$$\Omega_j(t)=\{\boldsymbol{r}\,|\,(\boldsymbol{r}-\boldsymbol{r}_j(t))A_j(t)(\boldsymbol{r}-\boldsymbol{r}_j(t))^T\leqslant 1,\quad \boldsymbol{r}\in\mathbb{R}^2\}, \tag{14)'}$$

where $A_j(t)=Z_j^{-1}(t)A_j(0)(Z_j^{-1}(t))^T$ and $A_j(0)$ is the initial coefficient matrix of ellipse Ω_j. In view of the proposition in Section 1 each of $\Omega_j(t)$ is preserved in elliptic shape and its area is conserved but its axis ratio and orientation may be changed in time. Systems (11) and (12) with (9) and (13) yield a time continuous semidiscrete simulation to the Euler equations (1) with second order accuracy in space. There are $6N$ equations (11), (12) with $6N$ unknowns $\boldsymbol{r}_j(t)$, $Z_j(t)$ $(j=1,\,2,\,\cdots,\,N)$.

Next we derive a full discrete version of the variable-elliptic-vortex method. For the sake of simplicity, equations (12) are approximated by Euler's method

$$\boldsymbol{r}_j^{n+1}=\boldsymbol{r}_j^n+\boldsymbol{u}(\boldsymbol{r}_j^n,\,nk)k, \tag{15}$$

where k is a time step, $\boldsymbol{r}_j^n=\boldsymbol{r}_j(nk)$ are the center coordinates of Ω_j^n and $\Omega_j^n=\Omega_j(nk)$.

To approximate (11) we freeze $\nabla \boldsymbol{u}(\boldsymbol{r}_j(t), t) = \nabla \boldsymbol{u}(\boldsymbol{r}_j^n, nk)$ in time interval $[nk, (n+1)k)$ and then we get a linear constant coefficient system

$$\begin{cases} \dfrac{dZ_j}{dt} = Z_j \cdot \nabla \boldsymbol{u}(\boldsymbol{r}_j^n, nk)^T, & t \in [nk, (n+1)k), \\ Z_j|_{t=nk} = E. \end{cases} \tag{16}$$

From O.D.E. we know that Z_j can be integrated in close form ([8]). In terms of $Z_j^{n+1} = Z_j((n+1)k)$ one gets

$$\Omega_j^{n+1} = \{\boldsymbol{r} \mid (\boldsymbol{r} - \boldsymbol{r}_j^{n+1}) A_j^{n+1} (\boldsymbol{r} - \boldsymbol{r}_j^{n+1})^T \leqslant 1, \quad \boldsymbol{r} \in \mathbb{R}^2\}, \tag{17a}$$

where

$$A_j^{n+1} = (Z_j^{n+1})^{-1} A_j^n ((Z_j^{n+1})^{-1})^T \tag{17b}$$

and $A_j^0 = A_j(0)$. In summary the procedure for mimioking equations (1) is as follows. The elliptic vortex blobs Ω_j^n are moved by the law (15) and deformed by the map (17), and then the new velocity field (9) at $t = (n+1)k$ is determined by the vortex blobs at their new positions $\boldsymbol{r}_j^{n+1}$ and in their new elliptic shapes Ω_j^{n+1}. Repeating the procedure (15) and (16) one gets an approximate solution of (1). Note that in the process of solving (15) and (16) one needs the expressions of $\boldsymbol{u}(\boldsymbol{r}_j^n, nk)$ and $\nabla \boldsymbol{u}(\boldsymbol{r}_j^n, nk)$ given in (9) and (13).

Finally we give a criterion of selecting time step k. Let us consider a special case where only one elliptic vortex blob $\xi_1 = \Gamma_1 \gamma(\boldsymbol{r}; \Omega_1)$ exists. When $N=1$ the velocity field (9) is a linear vector function of $\boldsymbol{r}$ for $\boldsymbol{r} \in \Omega_1(t)$, so that (14)′ gives the exact motion of $\Omega_1(t)$. Some calculation on (11) and (12) shows that the variable-elliptic-vortex method produces an exact solution of (1), the self rotation motion with a constant angular velocity

$$\omega_1 = \frac{\Gamma_1}{\pi(a_1+b_1)^2} \tag{18}$$

without change in its shape[9]. It is obvious for convergence requirement to restrict the rotation angle in one time step k to less than a given small angle, for example $\frac{\pi}{4}$, that is $k \leqslant \dfrac{\pi^2(a_1+b_1)^2}{4\Gamma_1}$ or $k \leqslant \dfrac{\pi^2 a_1 b_1}{2\Gamma_1}$. This suggests that in the general case k ought to satisfy

$$k \leqslant \frac{\pi^2}{4} \min_{1<j<N} \frac{(a_j+b_j)^2}{\Gamma_j} \tag{19a}$$

or

$$k \leqslant \frac{\pi^2}{2} \min_{1<j<N} \frac{a_j b_j}{\Gamma_j}. \tag{19b}$$

In the following calculations we choose k according to inequality (19b).

§ 4. Numerical Results

In this section we present some numerical experiments to demonstrate the performance of the variable-elliptic-vortex method.

1. Dynamic motion of two Rankine vortices. Suppose the two Rankine vortices have radius R, density Γ_0 and are placed at a distance D. We use two variable elliptic vortex blobs to simulate their motions. In order to keep this approximation

in a reasonably accurate regime R is not allowed to be too big and D not too small. In the calculation we choose $R=1$, $D=3.6$ and $\Gamma_0=1$. The time step is chosen to be $k=0.1$. Numerical results are displayed in Fig. 1. The patterns resemble the one given by the vortex-in-cell method in Christiansen [10], where they use a cloud of point vortices. From this example we can see how the elliptic vortex blobs are translated and deformed in time.

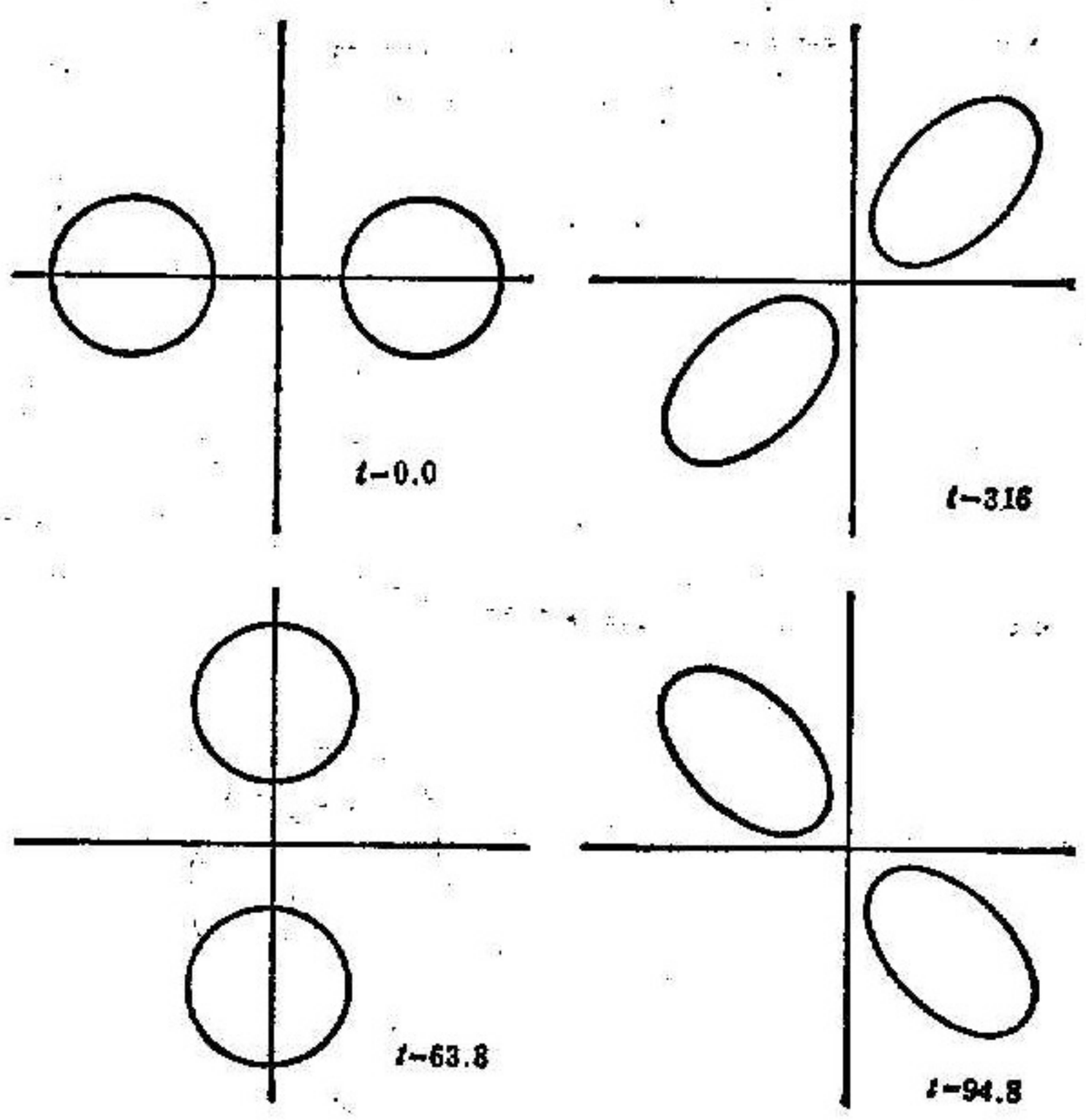

Fig. 1 Two vortices precessing around each other.

2. Rotation of a vortex sheet. The sheet is defined as the limit of an infinitely thin elliptic vortex with a uniform vorticity distribution. Therefore the initial vorticity distribution along the sheet is given by

$$\xi(x, y, 0) = (1-x^2)^{1/2}, \quad -1 \leqslant x \leqslant 1, \quad y=0.$$

It is known that the sheet rotates with a constant angular velocity $\omega=\frac{1}{2}$ without change in its length and its distribution ([9], [4]). We use the vortex method to approximate this problem, so that we can estimate its accuracy quantitatively. The sheet is replaced by a row of $N=30$ elliptic vortex blobs at equal distance apart. The initial vortex blobs are given by

$$(x_j^0, y_j^0) = \left(-1+\frac{1}{15}\left(j-\frac{1}{2}\right), 0\right), \quad A_j^0 = \begin{pmatrix} (0.0385)^{-2}, & 0 \\ 0, & (0.001)^2 \end{pmatrix},$$

$$\Gamma_j = \int_{x_j^0-\frac{1}{30}}^{x_j^0+\frac{1}{30}} (1-x^2)^{1/2}\,dx, \quad j=1, 2, \cdots, 30.$$

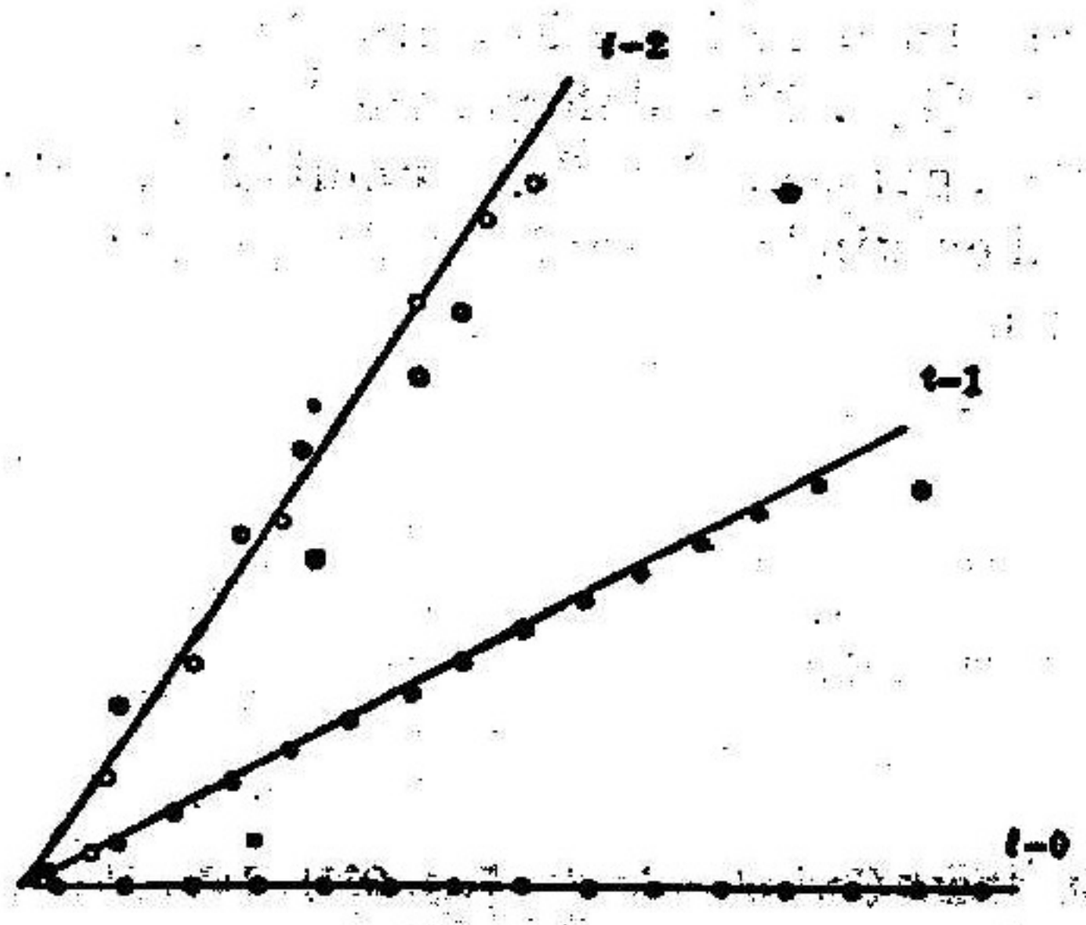

Fig. 2 Variable-elliptic-vortex approximation to the rotation of a vortex sheet.

The time step is $k=0.01$. The results are displaced in Fig. 2. By symmetry only a half of the blobs are shown in Fig. 2. The solid lines indicate the angle of rotation due to the exact solution. The periods and the small circles represent the centers of vortex blobs at different time. From Fig. 2 we can see the numerical solutions are in very close agreement with the exact solution at $t=1$ except for the end blobs. At $t=2$ the pattern becomes chaotic. This occurs because the sheet is an unstable rotation steady-state to infinitesimal perturbations ([11]) and the vortex method by its nature introduces finite-amplitude perturbations. This example shows the validity and the accuracy of this method.

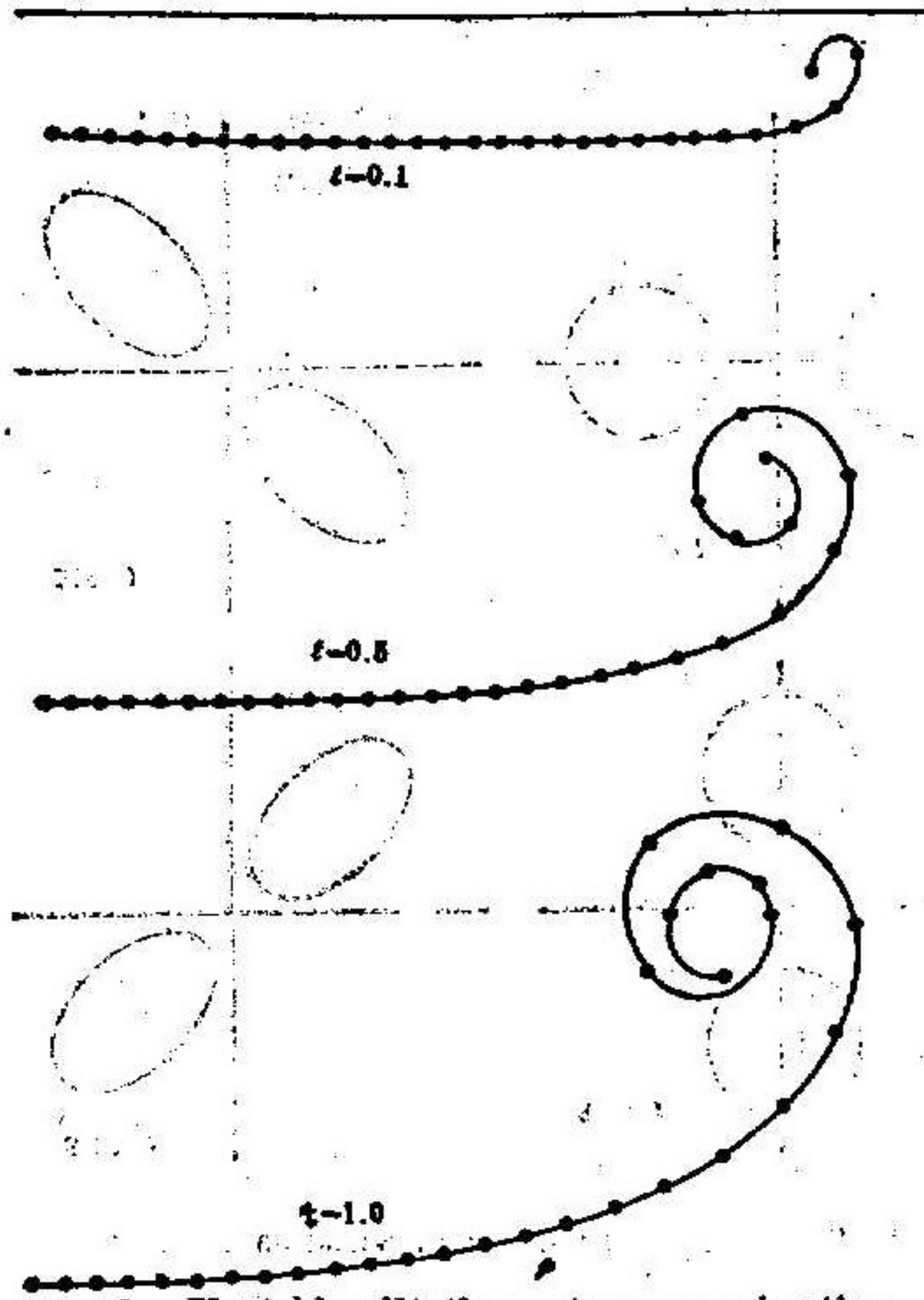

Fig. 3 Variable-elliptic-vortex approximation to the rolling-up of a vortex sheet.

3. Rolling-up of vortex sheet. We consider the vortex sheet of finite length with the following initial vorticity distribution

$$\xi(x, y, 0) = -\frac{d}{dx}(1-x^2)^{1/2},$$

$$-1 \leqslant x \leqslant 1,\ y = 0.$$

The sheet is approximated by a row of $N=60$ elliptic blobs at equal distance apart. The initial blobs are defined by

$$(x_j^0, y_j^0) = \left(-1+\frac{1}{30}\left(j-\frac{1}{2}\right), 0\right),$$

$$A_j^0 = \begin{pmatrix} (0.0192)^{-2}, & 0 \\ 0, & (0.0003)^{-2} \end{pmatrix},$$

$$\Gamma_j = (1-x^2)^{1/2}\Big|_{x_j^0-\frac{1}{60}}^{x_j^0+\frac{1}{60}},$$

$$j = 1, 2 \cdots, 60.$$

The time step is $k=0.01$. The results showed in Fig. 3 are reasonable in view of what is known from the numerical experiments in [12] and [4].

§ 5. Conclusion

We have presented a new variable-elliptic-vortex method for approximating incompressible inviscid fluid flows. Also, this method can be easily used to approximate high Reynolds number flow by incorporating a random walk algorithm to mimic the viscosity effect and a vortex generation algorithm to maintain the no-slip boundary condition (see Chorin [3], Teng [1]). The deformable behavior of elliptic-vortex blobs may provide a versatile approach for flow simulation. We expect that this method will be applied to other kinds of inviscid flow problems as well as high Reynolds number flow problems.

References

[1] Z. H. Teng, *J. Comput. Phys.*, **46** (1982), 54.
[2] L. Rosenhead, *Proc. Roy. Soc. London*, **A 134** (1931), 170.
[3] A. J. Chorin, *J. Fluid Mech.*, **57** (1973), 785.
[4] K. Kuwahara, H. Takami, *J. Phys: Soc. Japan*, **34** (1973), 247.
[5] A. Leonard, *J. Comput. Phys.*, **37** (1980), 289.
[6] O. Hald, *SIAM J. Numer. Anal.*, **16** (1979), 726.
[7] J. T. Beale, A. Majda, *Math. Comp.*, **39** (1982), 1.
[8] S. L. Ross, Introduction to Ordinary Differential Equations (3rd ed., Chapter 7, p. 265), John Wiley and Sons, New York, 1980.
[9] H. Lamb, Hydrodynamics (6th ed., Section 159, p. 232), Dover, New York, 1932.
[10] J. P. Christiansen, *J. Comput. Phys.*, **13** (1973), 363.
[11] A. E. H. Love, *Proc. London Math. Soc.*, (1), **25** (1893), 18.
[12] A. J. Chorin, P. S. Bernard, *J. Comput. Phys.*, **13** (1973), 423.
[13] P. A. Raviart, "An Analysis of Particle Methods", CIME Course in Numerical Methods in Fluid Dynamics, Como, July 1983.